

4000
8 SEP REC'D

NRL Report 8004

Effect of Section Size on the Fatigue Crack Growth Rate of A516-60 Pressure Vessel Steel

A. M. SULLIVAN AND T. W. CROOKER

*Strength of Metals Branch
Engineering Materials Division*

August 4, 1976

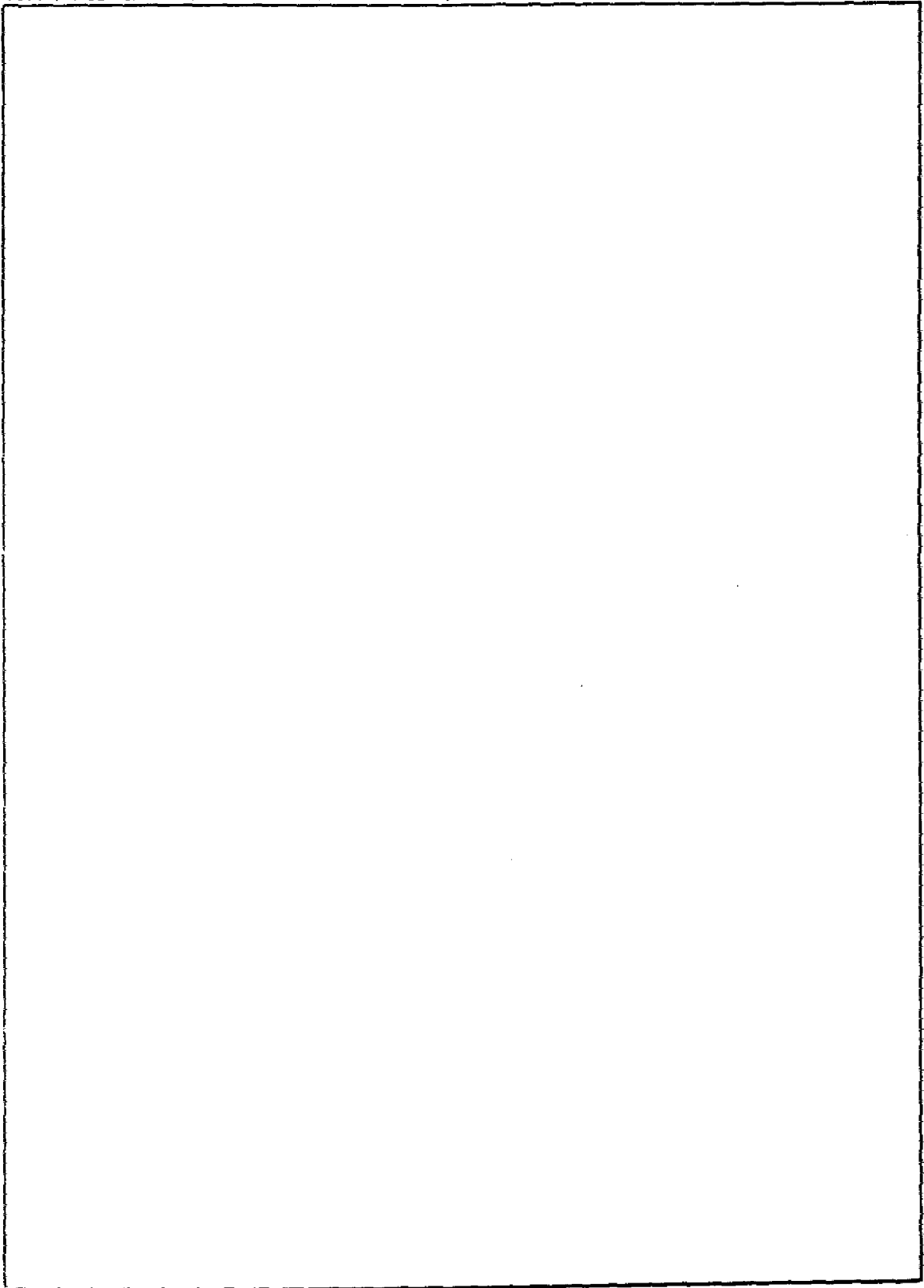


NAVAL RESEARCH LABORATORY
Washington, D.C.

Approved for public release: distribution unlimited.

REPORT DOCUMENTATION PAGE	
1. REPORT NUMBER NRL Report 8004	2.
4. TITLE (and Subtitle) EFFECT OF SECTION SIZE ON THE FATIGUE CRACK GROWTH RATE OF A516-60 PRESSURE-VESSEL STEEL	5. TYPE OF REPORT & PERIOD COVERED Final report on one phase of a continuing NRL Problem.
7. AUTHOR(s) A. M. Sullivan and T. W. Crooker	6. PERFORMING ORG. REPORT NUMBER
9. PERFORMING ORGANIZATION NAME AND ADDRESS Naval Research Laboratory Washington, D.C. 20375	8. CONTRACT OR GRANT NUMBER(s)
11. CONTROLLING OFFICE NAME AND ADDRESS Department of the Navy Office of Naval Research Arlington, Va. 22217	10. PROGRAM ELEMENT, PROJECT, TASK AREA & WORK UNIT NUMBERS NRL Problem MO1-24 RR 022-01-46-5431
14. MONITORING AGENCY NAME & ADDRESS (if different from Controlling Office)	12. REPORT DATE August 4, 1976
	13. NUMBER OF PAGES 17
	15. SECURITY CLASS. (of this report) Unclassified
	15a. DECLASSIFICATION/DOWNGRADING SCHEDULE
16. DISTRIBUTION STATEMENT (of this Report) Approved for public release; distribution unlimited.	
17. DISTRIBUTION STATEMENT (of the abstract entered in Block 20, if different from Report)	
18. SUPPLEMENTARY NOTES	
19. KEY WORDS (Continue on reverse side if necessary and identify by block number) Fatigue crack growth Pressure-vessel steel Section-size effects Specimen thickness	
20. ABSTRACT (Continue on reverse side if necessary and identify by block number) Studies of the fatigue crack growth rate of A516-60 pressure-vessel steel indicate no section-size effect in stress-relieved specimens ranging in thickness from 6.35-50.8 mm (0.25 to 2.0 in.). A regression curve equation for all thicknesses, relating cyclic crack growth rate (da/dN) to crack-tip stress-intensity factor range (ΔK) is obtained. The significance of these results is discussed in the light of current engineering practice and of previous studies of size effects in fatigue crack propagation.	

SECURITY CLASSIFICATION OF THIS PAGE(When Data Entered)



CONTENTS

INTRODUCTION	1
EXPERIMENTAL CONSIDERATIONS	2
DISCUSSION OF EXPERIMENTAL RESULTS	3
REGRESSION ANALYSIS	7
ESTIMATES FROM REGRESSION CURVE EQUATION	8
CONCLUSIONS	11
ACKNOWLEDGMENTS	11
REFERENCES	11
SYMBOLS	13

EFFECT OF SECTION SIZE ON THE FATIGUE CRACK GROWTH RATE OF A516-60 PRESSURE VESSEL STEEL

INTRODUCTION

A primary goal of structural design is to produce reliable structures that are as inexpensive as possible to fabricate and maintain. Achieving this requires a knowledge of the conditions giving rise to catastrophic fracture and governing subcritical crack growth. The applicability of linear elastic fracture mechanics (LEFM) to these design problems is now widely accepted, and the conditions giving rise to catastrophic fracture can be defined by the stress-intensity parameter K_{Ic} (plane strain) or K_c (plane stress).

Fatigue crack growth rate (da/dN) can also be related to the stress-intensity factor range ΔK . However, little is known about possible section-size effects in fatigue crack propagation. Because of this, and because generating data for specific cases is expensive and time-consuming, design engineers conducting crack growth analyses tend to extrapolate da/dN data to thinner or thicker sections as a routine engineering approximation. The current literature is of little help in judging the wisdom of these approximations, since the evidence for the effect of thickness on fatigue crack growth is conflicting.

In 1970, for example, Clark and Trout [1] observed faster crack growth in 25.4-mm-thick (1 in.) specimens of a Ni-Mo-V rotor forging than in 50.8-mm (2 in.) specimens. However, in a subsequent study on ASTM A533-B steel, Clark [2] found the fatigue crack growth rate (FCGR) to be essentially constant over a thickness range from 25.4 to 101.6 mm (1-4 in.).

Jack and Price [3] support the first conclusion with data from tests of mild steel specimens with thicknesses ranging from 1.27 to 22.9 mm (0.05-0.90 in.). The second is supported by Parry et al. [4] in ASTM A514 steel 1.55 to 6.73 mm (0.061-0.265 in.) thick; Hahn et al. [5] in 3% silicon ferrite 1.52 to 12.7 mm (0.06-0.50 in.) thick; and Griffiths and Richards [6].

Both conclusions are opposed by those of Barsom et al. [7], testing several high strength steels in 25.4 to 50.8-mm (1 and 2 in.) specimens, and Heiser and Mortimer [8], testing 4340 steel in thicknesses from 1.6 to 12.7 mm (0.0625-0.50 in.). These authors report increasing crack growth rates with increasing thickness.

Except for the study by Barsom et al., the thinner specimens were machined down from thicker parent material. Such a practice tends to increase data scatter and also to cause ambiguity in result interpretation. A recent study on 5Ni-Cr-Mo-V steel by Sullivan and Crooker [9] showed that unrelieved residual stresses caused significant scatter in da/dN data obtained from specimens cut down from 25.4-mm-thick (1 in.) as-rolled, quenched, and tempered plate. Stress-relieved specimens, on the other hand, indicated no effect of specimen thickness but did show an increased crack growth rate for all thicknesses studied.

To recapitulate, three types of response have been documented:

1. Crack growth accelerated by decreased thickness

Manuscript submitted March 31, 1976.

2. No effect of thickness
3. Crack growth accelerated by increased thickness.

Furthermore, factors other than thickness influence and cloud the results of section-size investigations.

Given this confused background, the present study was undertaken to explore systematically the effects of thickness and specimen size on the FCGR of a low-strength pressure-vessel steel, A516-60. This material is reasonably homogeneous in thicknesses up to 50.8 mm (2 in.) and can be stress-relieved without significantly altering its mechanical properties. Finally, both the steel itself and the specimen thicknesses investigated conform to a broad range of industrial uses.

EXPERIMENTAL CONSIDERATIONS

The A516-60 steel used for these investigations was 76.2 mm (3-in.) thick as rolled. It contained 0.17 wt% carbon and developed a yield stress of 43.7 ksi (301.3 MN/m²) after normalizing at 900°C (1,650°F). After machining, the specimens were further stress-relieved at 620°C (1,050°F) for 1 h. Compact tension (CT) specimens having the configuration recommended for a recent ASTM committee interlaboratory program [10] were used. Specimens designated as 1-T are illustrated in Fig. 1. They were tested in two thicknesses, 12.7 and 25.4 mm (0.50 and 1.00 in.). All planar dimensions of the 2-T specimens are twice those of Fig. 1; these were tested in four thicknesses, 6.4, 12.7, 25.4, and 50.8 mm (0.25, 0.50, 1.00, and 2.00 in.).

Fatigue testing was conducted under tension-tension cyclic loading using a haversine waveform on a 0.49-MN (110-kip) capacity MTS closed-loop testing machine. The cyclic frequency was 5 Hz, and the stress ratio R was 0.10. Crack-length measurements were made using a crack-opening-displacement (COD) technique [11]. A commercial MTS COD clip gage was used, the notched arms of which fit over knife edges screwed onto the specimen to straddle the mouth of the machined notch. Signals from the COD strain gage circuit were fed into a Hewlett-Packard XY recorder, together with those from the load cell of the testing machine, to give a series of stress-COD curves.

Two specimens were tested at each thickness, with loads chosen to give predetermined ΔK values, to provide a region of overlap in the (da/dN) -vs- ΔK plots.

Crack length was determined by reference to the EB [COD]/P-vs-a/W calibration curve, for which a polynomial expression has been developed. Details of this technique are available [12]. Crack-growth rate da/dN was determined by fitting tangents to the a-vs-N curves using a Bausch and Lomb split-prism tangent meter. The stress-intensity factor range ΔK is computed from the expression

$$\Delta K = \Delta \sigma \sqrt{a} Y \quad (1)$$

where

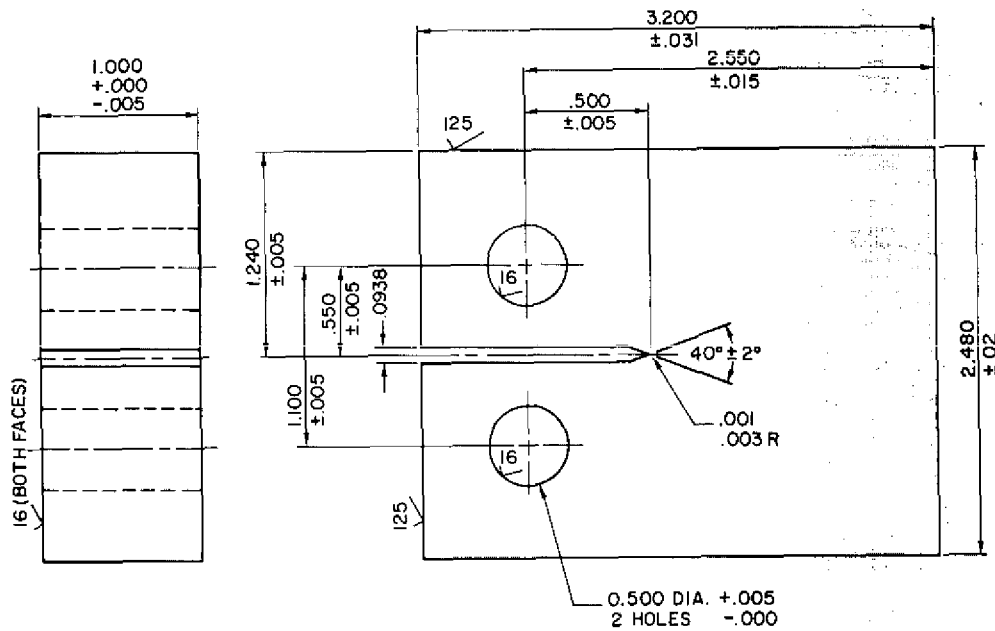


Fig. 1 — 1-T compact tension specimen with $h/W = 0.486$

$$Y = 30.96 - 195.8 (a/W) + 730.6 (a/W)^2 - 1186.3 (a/W)^3 + 754.6 (a/W)^4.$$

This polynomial is appropriate for the 0.486 height-to-width ratio h/W of the specimen [13]. A stress-range normalizing factor is used, such that

$$\Delta K_{\text{eff}} = [(1-bR)/(1-R)] \Delta K \quad (2)$$

where, for the positive values of R in this material, $b = 0.85$. Data are contained in Tables 1 through 4. All specimens were loaded in tension to failure at the conclusion of the FCGR test.

DISCUSSION OF EXPERIMENTAL RESULTS

Figures 2a, 2b, and 2c show that there is essentially no difference in measured FCGR between the 1-T and 2-T specimens, although the latter exhibit somewhat more data scatter. Further, no discernible effect of thickness can be observed. The trend line shown on each curve was developed from regression analyses of all specimens (288 pairs of data points).

Although an ASTM thickness restriction for K_{Ic} test specimens is specified [14] according to the equation

SULLIVAN AND CROOKER

Table 1 -- A516-60 Steel, (1-T Specimen, $\Delta\sigma = 1.740$ ksi)

Crack Length, a (in.)	ΔK_{eff} (ksj/ $\sqrt{in.}$)	Specimen No. 864 Specimen Thickness B, 0.50 in. (12.7mm) da/dN ($\times 10^{-6}$)	Specimen No. 866 Specimen Thickness B, 1.00 in. (25.4mm) da/dN ($\times 10^{-6}$)
0.825	19.6	2.66	2.33
0.850	20.0	2.77	3.18
0.875	20.4	3.04	3.37
0.900	20.8	3.24	3.50
0.925	21.2	3.50	3.70
0.950	21.7	3.63	3.90
0.975	22.2	3.91	4.20
1.000	22.7	4.50	4.34
1.025	23.2	4.86	4.72
1.050	23.7	5.08	4.91
1.075	24.2	5.27	5.25
1.100	24.8	5.75	5.65
1.125	25.3	6.06	5.96
1.150	25.9	6.46	6.52
1.175	26.5	6.64	6.96
1.200	27.1	7.32	7.41
1.225	27.7	7.52	8.00
1.250	28.4	8.52	9.21
1.275	29.1	9.50	9.81
1.300	29.8	10.02	10.72
1.325	30.6	10.72	11.78
1.350	31.4	12.38	13.74
1.375	32.4	13.74	15.76
1.400	33.3	14.86	18.66

Table 2 -- A516-60 Steel, (1-T Specimen,
 $\Delta\sigma = 2.740$ ksi)

Crack Length, a (in.)	ΔK_{eff} (ksj/ $\sqrt{in.}$)	Specimen No. 865 Specimen Thickness B, 0.50 in. (12.7mm) da/dN ($\times 10^{-6}$)	Specimen No. 867 Specimen Thickness B, 1.00 in. (25.4mm) da/dN ($\times 10^{-6}$)
0.825	30.8	11.86	12.50
0.850	31.4	12.28	13.08
0.875	32.1	12.94	14.90
0.900	32.8	13.98	15.66
0.925	33.4	15.32	16.17
0.950	34.2	16.58	16.58
0.975	35.0	17.20	17.21
1.000	35.8	18.12	17.98
1.025	36.5	18.67	18.53
1.050	37.3	19.62	19.62
1.075	38.2	20.80	20.80
1.100	39.0	21.65	22.55
1.125	39.8	23.02	23.51
1.150	40.8	23.91	24.53
1.175	41.8	25.62	25.62
1.200	42.7	28.08	28.08
1.225	43.7	29.44	29.44
1.250	44.8	30.94	30.94
1.275	45.8	32.56	34.34
1.300	47.0	37.14	38.47
1.325	48.2	39.41	40.88
1.350	49.5	43.56	45.07
1.375	50.9	46.65	50.14
1.400	52.4	54.14	54.14

Table 3 — A516-60 Steel, (1-T Specimen, $\Delta\sigma = 1.228$ ksi)

Crack Length, a (in.)	ΔK_{eff} (ksi $\sqrt{in.}$)	Specimen No. 871 Specimen Thickness B, 0.25 in. (6.4mm) da/dN ($\times 10^{-6}$)	Specimen No. 870 Specimen Thickness B, 0.50 in. (12.7mm) da/dN ($\times 10^{-6}$)	Specimen No. 872 Specimen Thickness B, 1.00 in. (25.4mm) da/dN ($\times 10^{-6}$)	Specimen No. 876 Specimen Thickness B, 2.00 in. (50.8mm) da/dN ($\times 10^{-6}$)
1.650	19.5	1.92	2.07	2.44	2.22
1.700	19.9	2.12	2.22	3.00	2.54
1.750	20.3	2.33	2.54	3.24	2.71
1.800	20.8	2.71	2.88	3.50	2.94
1.850	21.2	3.12	2.82	3.63	3.06
1.900	21.6	3.24	3.37	3.76	3.37
1.950	22.2	3.50	3.63	3.91	4.04
2.000	22.6	3.76	3.76	4.20	4.34
2.050	23.2	3.91	4.04	4.42	4.74
2.100	23.6	4.04	4.42	4.82	5.26
2.150	24.2	4.34	4.66	5.18	5.55
2.200	24.6	4.66	5.00	5.55	6.17
2.250	25.2	5.00	5.55	6.24	6.64
2.300	25.8	5.25	5.75	6.64	7.14
2.350	26.4	5.75	6.24	7.14	7.70
2.400	27.0	6.24	6.88	7.60	8.32
2.450	27.6	6.88	7.41	8.32	9.02
2.500	28.4	7.41	8.00	9.25	9.66
2.550	29.0	8.00	8.66	10.02	9.81
2.600	29.8	8.66	9.81	11.23	11.20
2.650	30.6	9.61	11.23	13.26	11.78
2.700	31.4	10.25	13.02	14.52	12.38
2.750	32.2	11.78	14.52	16.35	13.02
2.800	33.2	12.38	17.44	21.66	14.52

Table 4 -- A516-60 Steel, (2-T Specimen, $\Delta\sigma = 1.932$ ksi)

Crack Length, a (in.)	ΔK_{eff} (ksi $\sqrt{in.}$)	Specimen No. 873 Specimen Thickness B, 0.25 in. (6.4mm) da/dN ($\times 10^{-6}$)	Specimen No. 874 Specimen Thickness B, 0.50 in. (12.7mm) da/dN ($\times 10^{-6}$)	Specimen No. 875 Specimen Thickness B, 1.00 in. (25.4mm) da/dN ($\times 10^{-6}$)	Specimen No. 877 Specimen Thickness B, 2.00 in. (50.8mm) da/dN ($\times 10^{-6}$)
1.650	30.6	9.08	10.68	12.07	9.76
1.700	31.3	9.59	11.41	12.50	10.48
1.750	32.0	10.12	11.66	12.50	11.82
1.800	32.6	10.86	12.50	13.12	12.50
1.850	33.3	11.26	14.38	13.54	13.54
1.900	34.1	12.07	16.77	13.88	13.88
1.950	34.8	12.94	17.52	14.64	14.12
2.000	35.6	14.38	17.52	15.44	14.90
2.050	36.4	16.29	18.05	16.23	15.44
2.100	37.2	17.21	18.53	16.73	16.00
2.150	38.0	17.85	19.47	17.85	16.89
2.200	38.8	18.53	21.00	19.24	17.85
2.250	39.7	19.62	22.09	20.80	19.03
2.300	40.6	20.80	24.22	21.65	20.80
2.350	41.5	23.02	25.62	23.31	22.55
2.400	42.5	24.53	28.08	24.74	24.53
2.450	43.4	26.81	30.18	27.30	25.62
2.500	44.6	29.93	31.73	29.44	27.30
2.550	45.6	32.56	35.04	31.73	29.44
2.600	46.8	34.34	39.64	37.36	30.94
2.650	48.1	38.47	43.59	39.64	36.30
2.700	49.3	44.47	50.14	46.65	45.07
2.750	50.7	50.14	60.36	52.88	50.14
2.800	52.2	64.31	70.89	67.44	56.38

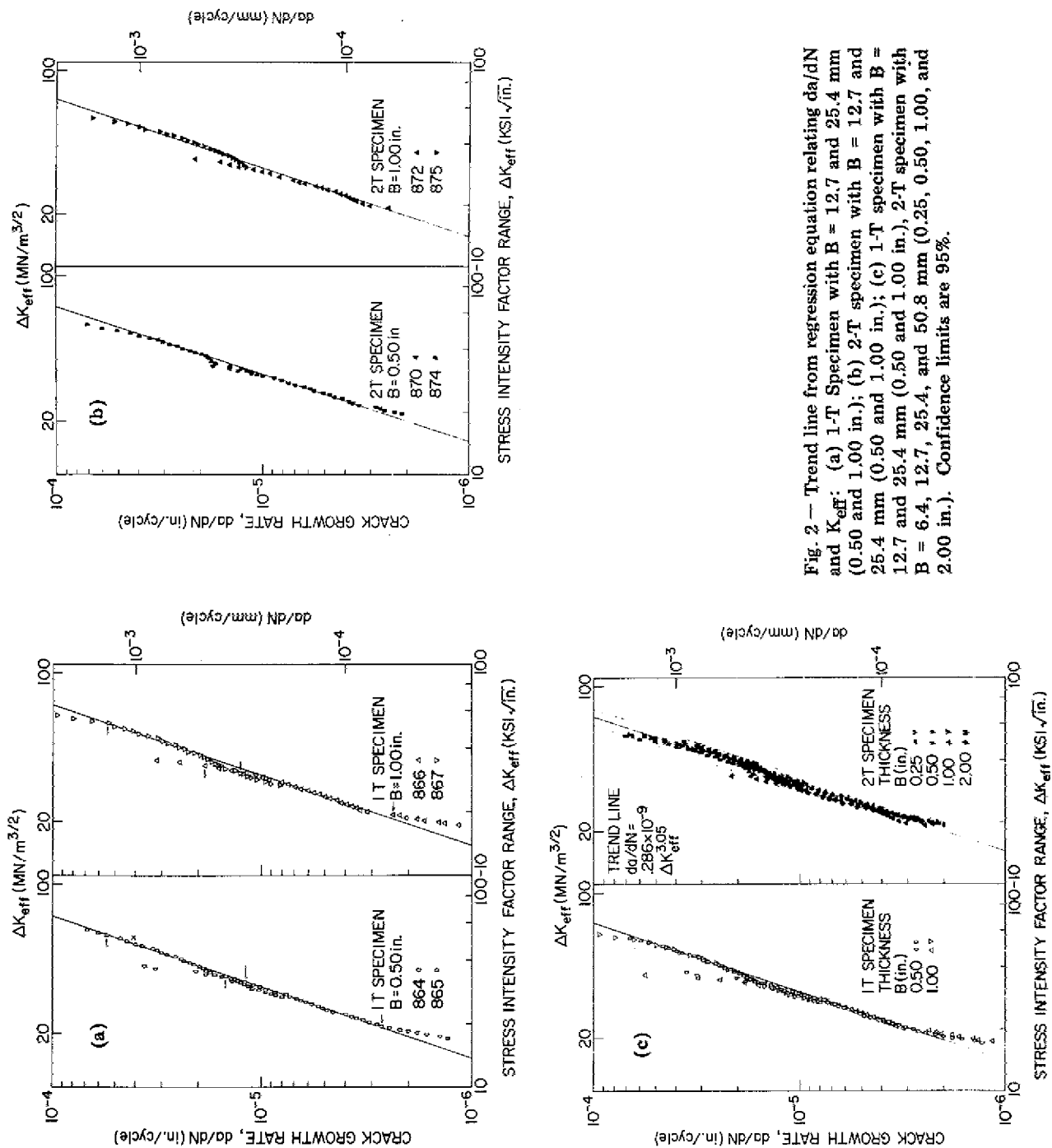


Fig. 2 — Trend line from regression equation relating da/dN and K_{eff} : (a) 1-T Specimen with B = 12.7 and 25.4 mm (0.50 and 1.00 in.); (b) 2-T specimen with B = 12.7 and 25.4 mm (0.50 and 1.00 in.); (c) 1-T specimen with B = 12.7 and 25.4 mm (0.50 and 1.00 in.), 2-T specimen with B = 6.4, 12.7, 25.4, and 50.8 mm (0.25, 0.50, 1.00, and 2.00 in.). Confidence limits are 95%.

$$B = 2.5 \left(\frac{K_{\max}}{\sigma_{ys}} \right)^2 = \left(\frac{\Delta K}{(1-R)\sigma_{ys}} \right)^2, \quad (3)$$

its application to the ΔK values employed for fatigue crack propagation seems unwarranted, since data for all thicknesses conform well to a regression equation between values of ΔK from 22 to 55 MN/m^{3/2} (20 to 50 ksi√in.). Table 5 contains values of limiting ΔK values obtained from Eq. (3).

Table 5 — Restricted Values of ΔK

Thickness, B (in.)	(MNm ^{3/2})	(ksi√in.)
0.25	13.3	12.1
0.50	19.0	17.3
1.00	26.8	24.4
2.00	38.0	34.6

No valid K_{Ic} data were obtained from the specimens loaded to failure. However, in thin-sheet testing, K values calculated from the stress measured at the departure from linearity (DL) of the elastic σ -COD line, although a little higher than the true K_{Ic} values for two aluminum alloys, discriminated between them appropriately [15]. Therefore, K_{DL} values were determined for this steel and are plotted in Fig. 3. Despite the low material yield strength, these K_{DL} values are low enough to be in the range of the regression-equation data. For this steel, perhaps the terminal stress intensity is K_{c} , that for plane stress, even though all specimens exhibited flat fracture.

A limited fractographic study shows the dominant mechanism of crack growth to be ductile striation formation. This supports the hypothesis of Richards and Lindley [16], who contend that this mechanism precludes specimen thickness effects.

However, recent studies have shown that mean stress [17] or an aqueous environment [18] can alter the mechanism of crack growth in a given material. It is therefore possible that under conditions promoting crack-tip constraints, and thereby a microcleavage crack growth mechanism, size effects not apparent in this investigation could be introduced.

REGRESSION ANALYSIS

Regression analyses for various combinations of the experimental data were developed in the linear form of

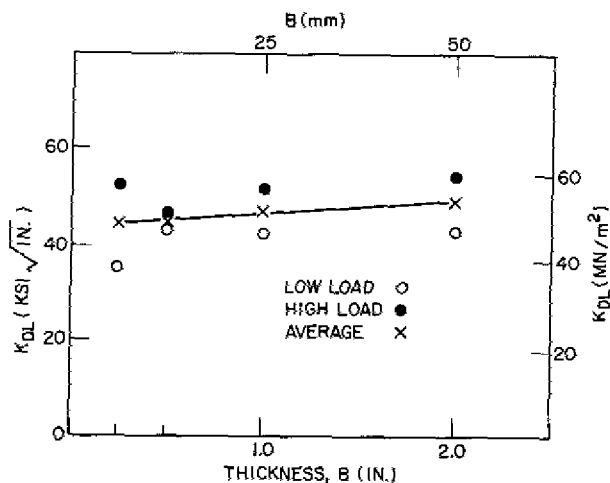


Fig. 3 — K_{DL} vs specimen thickness

$$\log_{10}^6 da/dN = n (\log_{10}^6 \Delta K_{eff}) + \log_{10}^6 A \quad (4)$$

and transformed to the familiar exponential equation

$$da/dN = A \Delta K_{eff}^n \quad (5)$$

The regression curve equation for all thicknesses of both 1-T and 2-T specimens was calculated to be

$$da/dN = 0.286 \times 10^{-9} \Delta K_{eff}^{3.06} \quad (6)$$

A correlation coefficient of $r_{xy} = 0.991$ was obtained with this equation. Values of the exponent n , correlation coefficient r_{xy} , and percent of twice the standard error of estimate (95% confidence limits) are shown in Figs. 4, 5, and 6. Slightly more scatter was evident as thickness or specimen size increased. It is uncertain whether this trend would persist in larger specimens or structures subjected to cyclic loadings, or tend to level off as indicated by the 2-T specimens of Fig. 7.

ESTIMATES FROM REGRESSION CURVE EQUATION

The value of any FCGR trend-line equation lies in its ability to predict crack growth. The close correlation between the data curves of crack length a vs number of cycles N and the curves estimated from the regression equation is seen in Figs. 7a and 7b. Scatter bands of $\pm 10\%$ and $\pm 15\%$ enclose, respectively, data from the 1-T and 2-T specimens.

Fig. 4 — Regression equation exponent n vs thickness and specimen size

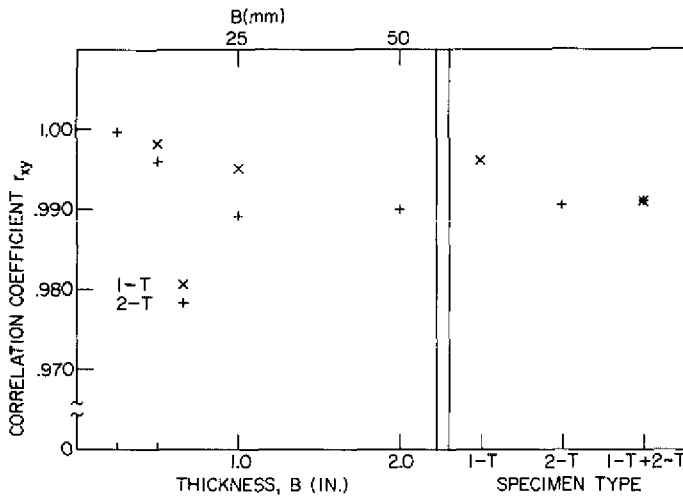
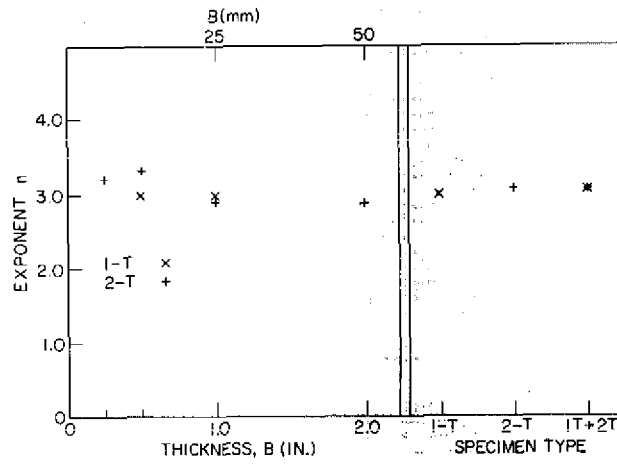


Fig. 5 — Correlation coefficient r_{xy} (for regression equations) vs thickness and specimen size. Asterisk represents all thickness values.

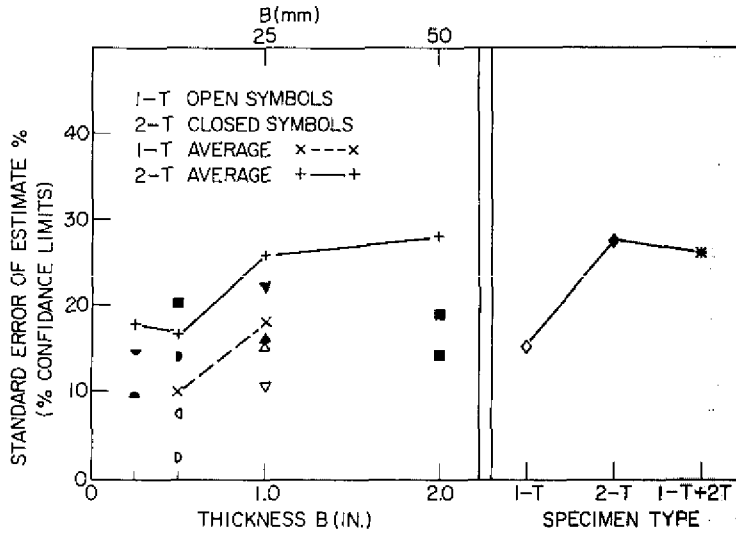


Fig. 6 — Standard error of estimate in percent vs thickness (x represents 1-T average, + represents 2-T average) and specimen size (asterisk represents all values of thickness)

CONCLUSIONS

- Neither size nor thickness of the specimen affect the fatigue crack growth rate observed in stress-relieved specimens of ASTM A516-60 steel cut down from an as-rolled and normalized 76.2-mm (3-in.) plate.
- Curves of crack length vs number of cycles estimated from the crack growth rate regression equation agree well with actual data curves.
- An increase in data scatter is noted with increased thickness and size.
- No effect of crack-tip stress state, as defined by the ASTM testing limit for plane strain fracture toughness, was observed in this study.
- No broader generalizations can be made concerning the effect of section size on fatigue crack growth rate without further systematic testing of a variety of materials under varied conditions.
- For fail-safe design, at present, conservative practice indicates the necessity of testing material in both the thinnest and the thickest sections exactly as they are to be encountered in the structure, i.e., as-rolled, cut-down, heat-treated, stress-relieved, etc.

ACKNOWLEDGMENTS

The financial support of the Office of Naval Research is gratefully acknowledged. Invaluable experimental assistance was provided by M. Cigledy.

REFERENCES

1. W.G. Clark, Jr., and H.E. Trout, Jr., "Influence of Temperature and Section Size on Fatigue Crack Growth Behavior in Ni-Mo-V Alloy Steel," *Eng. Fracture Mech.* **2** (2), 107-123 (Nov. 1970).
2. W.G. Clark, Jr., "Effect of Temperature and Section Size on Fatigue Crack Growth in Pressure Vessel Steel," *J. Mater.* **6** (1), 134-149 (Mar. 1971).
3. A.R. Jack and A.T. Price, "Effects of Thickness on Fatigue Crack Initiation and Growth in Notched Mild Steel Specimens," *Acta Metall.* **20** (7), 857-866 (July 1972).
4. M. Parry, H. Nordberg, and R.W. Hertzberg, "Fatigue Crack Propagation in A514 Base Plate and Welded Joints," *J. Welding, Res. Suppl.* **51** (10), 485-s-490-s (Oct. 1972).
5. G.T. Hahn, R.G. Hoagland, and A.R. Rosenfield, "Local Yielding Attending Fatigue Crack Growth," ARL 71-0234, Air Force Systems Command, Aerospace Research Laboratories, Wright-Patterson AFB, Ohio, Nov. 1971.

6. J.R. Griffiths and C.E. Richards, "The Influence of Thickness on Fatigue Crack Propagation Rates in a Low Alloy Steel Weld Metal Above and Below General Yield," Mater. Sci. Eng. 11 (6), 305-310 (June 1973).
7. J.M. Barsom, E.J. Imhof, and S.T. Rolfe, "Fatigue-Crack Propagation in High Yield-Strength Steels," Eng. Fracture Mech. 2 (4), 301-317 (June 1971).
8. F.A. Heiser and W. Mortimer, "Effect of Thickness and Orientation on Fatigue Crack Growth Rate in 4340 Steel," Met. Trans. 3, 2119-2123 (1972).
9. A.M. Sullivan and T.W. Crooker, "The Effect of Specimen Thickness on Fatigue Crack-Growth-Rate in 5 Ni-Cr-Mo-V Steel—Comparison of Heat-Treated and Stress-Relieved Specimens," NRL Report 7936, Dec. 9, 1975.
10. W.G. Clark, Jr., and S.J. Hudak, Jr., "Variability in Fatigue Crack Growth Rate Testing," J. Testing Evaluation 3 (6), 454-476 (Nov. 1975).
11. A.M. Sullivan, "Crack-Length Determination for the Compact Tension Specimen Using a Crack-Opening-Displacement Calibration," NRL Report 7888, June 24, 1975.
12. A.M. Sullivan and T.W. Crooker, "Evaluation of Fatigue Crack-Growth-Rate Determination Using a Crack-Opening-Displacement Technique for Crack-Length Measurement," NRL Report 7912, Sept. 12, 1975.
13. E.T. Wessel, "State of the Art of the WOL Specimen for K_{Ic} Fracture Toughness Testing," Eng. Fracture Mech. 1 (1), 77-1030 (June 1968).
14. "Standard Method of Test for Plane Strain Fracture Toughness of Metallic Materials," E399 - Annual Book of ASTM Standards, Part 10, ASTM, Philadelphia, 1975, pp. 561-580.
15. A.M. Sullivan and C.N. Freed, "The Influence of Geometric Variables on K_c Values for Two Thin Sheet Aluminum Alloys," NRL Report 7270, June 17, 1971.
16. C.E. Richards and T.C. Lindley, "The Influence of Stress Intensity and Microstructure on Fatigue Crack Propagation in Ferritic Materials," Eng. Fracture Mech. 4 (4), 951-978 (1972).
17. C.J. Beevers, R.J. Cooke, J.F. Knott, and R.O. Ritchie, "Some Considerations of the Influence of Sub-Critical Cleavage Growth During Fatigue-Crack Propagation in Steels," Metal Sci. 9 (3), 119-126 (Mar. 1975).
18. O. Vosikovsky, "Fatigue-Crack Growth in an X-65 Line-Pipe Steel at Low Cyclic Frequencies in Aqueous Environments," Trans. ASME J. Eng. Mater. Technol. 97, Series H, No. 4, 298-304 (Oct. 1975).

SYMBOLS

a	crack length of CT specimen
a/W	crack length-to-width ratio
B	specimen thickness
COD	crack opening displacement
CT	compact tension specimen
da/dN	crack growth rate; change in crack length per cycle
E	Young's modulus
FCGR	fatigue crack growth rate
h	half-height of CT specimen
K_c	critical stress intensity parameter for plane stress
K_{DL}	K computed from stress value at the departure from linearity of a σ versus COD curve of a specimen loaded to fracture
K_{Ic}	critical stress-intensity parameter for plane strain
LEFM	linear elastic fracture mechanics
N	number of cycles
n	slope value of da/dN vs ΔK
P	load on specimen
R	stress ratio ($\sigma_{min}/\sigma_{max}$)
r_{xy}	correlation coefficient
W	specimen width
ΔK	stress-intensity parameter range ($K_{max} - K_{min}$)
ΔK_{eff}	stress-intensity parameter normalized for stress ratio effect; = $(1-bR/1-R) \Delta K$; where $R = +$, $b = 0.85$
σ	gross or nominal stress (P/BW)

σ_{\max} stress at maximum load
 σ_{\min} stress at minimum load
 σ_{ys} yield strength
 $\Delta\sigma$ stress range ($\sigma_{\max} - \sigma_{\min}$)

SYMBOLS

a	crack length of CT specimen
a/W	crack length-to-width ratio
B	specimen thickness
COD	crack opening displacement
CT	compact tension specimen
da/dN	crack growth rate; change in crack length per cycle
E	Young's modulus
FCGR	fatigue crack growth rate
h	half-height of CT specimen
K_c	critical stress intensity parameter for plane stress
K_{DL}	K computed from stress value at the departure from linearity of a σ versus COD curve of a specimen loaded to fracture
K_{Ic}	critical stress-intensity parameter for plane strain
LEFM	linear elastic fracture mechanics
N	number of cycles
n	slope value of da/dN vs ΔK
P	load on specimen
R	stress ratio ($\sigma_{min}/\sigma_{max}$)
r_{xy}	correlation coefficient
W	specimen width
ΔK	stress-intensity parameter range ($K_{max} - K_{min}$)
ΔK_{eff}	stress-intensity parameter normalized for stress ratio effect; = $(1-bR/1-R) \Delta K$; where R = +, b = 0.85
σ	gross or nominal stress (P/BW)

σ_{\max} stress at maximum load

σ_{\min} stress at minimum load

σ_{ys} yield strength

$\Delta\sigma$ stress range ($\sigma_{\max} - \sigma_{\min}$)